



Inkjet Printing of Zirconia: Coffee Staining and Line Stability

Journal:	<i>Journal of the American Ceramic Society</i>
Manuscript ID:	Draft
Manuscript Type:	Article
Date Submitted by the Author:	n/a
Complete List of Authors:	Dou, Rui; The University of Manchester, Materials Science Centre Wang, Tianming; University of Manchester, School of Materials Guo, Yunshan; University of Manchester, School of Materials Derby, Brian; University of Manchester, School of Materials
Keywords:	ink-jet, printing, zirconia, suspensions, drying

SCHOLARONE™
Manuscripts

view

Inkjet Printing of Zirconia: Coffee Staining and Line Stability

Rui Dou, Tianming Wang, Yunshan Guo and Brian Derby

School of Materials, University of Manchester,
Oxford Road, Manchester, M13 9PL, UK

Abstract

We have prepared a 10 vol % zirconium oxide powder aqueous ink for inkjet printing. This ink shows severe segregation or coffee staining during drying on solid substrates. Coffee staining is suppressed by the addition of 10 wt % PEG to the ink formulation. However, coffee staining occurs with the PEG solution ink when drops are printed onto a substrate made from a pre-printed ZrO_2 powder substrate. The mechanism for this phenomenon is not known but may be related to the draining of solvent into the powder. The stability of printed features is controlled by the overlap of printed drops and the range of line stability is shown to be consistent with models in the literature.

Introduction

Inkjet printing has great potential in a number of areas of materials manufacture such as: ceramic fabrication,¹ functional polymers and devices,² biomaterials and tissue engineering.³ Inkjet printing is now a mature technology with many years of applications in conventional digital printing and graphics output. However, there is an important distinction between these traditional uses of inkjet printing and its current application in materials fabrication. Digital printing aims to form a pixelated image on a planar substrate. This is achieved by printing individual arrays of dots of dye or pigment that remain isolated as they dry to ensure fidelity of the image. In contrast, materials manufacture normally aims to fabricate continuous features with 1- 2- or 3-dimensional connectivity and this is achieved by the interaction of printed drops, often in liquid form, to obtain the desired features.⁴ Hence an important aspect of inkjet printing of ceramics is the interaction of liquid drops deposited on planar surfaces to form stable features prior to drying or solidification of the drops.

In order to fabricate ceramic parts by inkjet printing, an appropriate precursor material must be delivered in a liquid form. Previous studies have shown that fine ceramic powders can be dispersed in an appropriate liquid to make inks suitable for inkjet printing.^{1,5-8} Typically, these inks dry by evaporation and contain about 5-10% solids by volume. Although it is also possible to use inks that solidify by a temperature induced phase change,⁹ the majority of published work using inkjet printing of ceramic powders has used an evaporating solvent,¹⁰ mainly because this method leads to high density powder compacts and reduced dimension change during subsequent sintering. However, during the drying of drops containing particles in suspension solute flows may occur and these can result in non-uniform deposition of solid. This

1
2
3 leads to preferential deposition along the contact line that defines the outer perimeter
4 of the drop. This phenomenon, which is also observed with the deposition of materials
5 from solution, is generally known as coffee staining.
6
7
8
9

10
11
12 The mechanisms of coffee staining were first explored by Deegan *et al*, who
13 attributed this phenomenon to the geometrical constraint of the pinned contact line of
14 a drying droplet.^{11,12} The radius of the droplet footprint on the surface does not shrink
15 during drying process because of contact line pinning. Hence the suspension/solution
16 must flow from the droplet centre to perimeter to compensate for evaporative losses.
17
18 The resulting outward flow can carry virtually all the material to the perimeter, where
19 it is deposited from the solvent to form the ring-like deposit. Under appropriate
20 conditions, coffee staining can result in extreme variations in deposit thickness and
21 this has been exploited to form individual ceramic wells.¹³ In order to produce well
22 defined objects by inkjet printing, it is necessary to control the coffee stain
23 phenomenon and produce homogeneous uniform dried drops. However, it is
24 interesting to note that the contact line pinning, which leads to coffee staining is an
25 important stabilising influence that allows the coalescence of droplets to form well
26 defined surface features.¹⁴ Thus methods of controlling coffee staining must maintain
27 the stability of liquid deposits prior to drying.
28
29
30
31
32
33
34
35
36
37
38
39
40
41
42
43
44
45
46
47
48
49

50 One mechanism by which coffee staining can be controlled is through the use of
51 solvent mixtures.¹⁵ Evaporation is enhanced at the edge of a drying drop because of
52 the presence of the surrounding region of dry substrate. When a droplet contains two
53 solvents with different evaporation rates, the solvent with the lowest evaporation rate
54 will be enriched at the edge of the droplet as drying progresses. If the solvent mixture
55
56
57
58
59
60

1
2
3 is selected such that the lower vapour pressure solvent has a smaller surface tension,
4
5 the concentration gradient resulting from the differential evaporation rates will lead to
6
7 a gradient in surface tension that generates a flow, known as a Marangoni flow,
8
9 opposing the flow generated by contact line pinning. The importance of these
10
11 Marangoni flows during droplet drying can be estimated using the dimensionless
12
13 Marangoni number, Ma , defined:
14
15
16

$$Ma = \frac{\Delta\gamma r}{\eta D} \quad (1)$$

17
18
19 where, $\Delta\gamma$ is the difference in surface tension (taken here to be the difference between
20
21 the two pure solvents), r is a characteristic length (assumed to be the radius of the
22
23 spread drop on the substrate), η is the fluid viscosity and D is the solute diffusion
24
25 coefficient. It is generally believed that Marangoni flows are significant if $Ma > 100$.
26
27
28
29
30
31
32
33

34 Here we present a study of the behaviour of an aqueous ZrO_2 ink after inkjet printing.
35
36 We explore the conditions under which stable individual lines are formed from the
37
38 coalescence of drops and further investigate whether these are consistent with models
39
40 developed for the inkjet printing of other fluids. The mechanisms of coffee staining
41
42 are explored on both solid substrates and when drops are deposited on dried ceramic
43
44 layers as is needed to produce 3-D objects through sequential overprinting.
45
46
47
48
49
50

51 **Experimental Materials and Methods**

52 Zirconium oxide powder with specific surface area = $7 \text{ m}^2\text{g}^{-1}$ and mean particle
53
54 diameter < 200 nm (99.99% Tosoh-Zirconia, T2-3YS-E, Tosoh Corporation,
55
56 Yamagushi, Japan) was used to prepare aqueous inks. A mixture of two different
57
58 surfactants was chosen to disperse the zirconium oxide powder in water: DISPEX
59
60

1
2
3 A40 (Ciba Specialty Chemicals Inc., Basel, Switzerland), and carboxylic acid
4 prepared DOLAPIX CE 64 (Zshimmier & Schwarz, Rhein, Germany). The inks were
5
6 mixed in polyethylene bottles with appropriate quantities of the surfactant by a
7
8 traditional ball milling process using ZrO₂ milling media for up to 7 days. In order to
9
10 investigate the effect of solvent mixtures on coffee staining, inks were also made with
11
12 aqueous solvents containing 10 wt % ethanol or 10 wt % poly(ethylene glycol) - PEG
13
14 (BDH, Poole, UK).
15
16
17
18
19
20
21

22 Suspension stability was assessed visually by leaving samples in cylindrical glass
23
24 vessels and examining them for sedimentation at regular intervals. Suspension
25
26 viscosity was measured using a concentric cylinder rheometer (RSIII, Brookfield,
27
28 Middleboro, MA, USA). The contact angle (as defined by the Young equation) of the
29
30 fluid on a range of substrates was determined by sessile drop experiments. Fluid
31
32 surface tension was measured using a pendant drop method. In both cases the
33
34 resulting drops were examined using image analysis software (FTA 200, Camtel,
35
36 Royston, U.K.).
37
38
39
40
41
42

43 Zirconia suspensions were printed onto clean substrates using an in house designed
44
45 and built laboratory scale inkjet printing platform that has a positional accuracy of 3
46
47 μm (Micromech Systems, Braintree, UK). This is equipped with piezoelectric
48
49 actuated inkjet printheads of internal diameter 60 μm (MJ-ATP-01, Microfab
50
51 Technologies, Plano, TX, USA) with drive electronics (JetDrive III, Microfab)
52
53 interfaced to a PC and controlled in a LabVIEW™ (National Instruments, Austin, TX,
54
55 USA) environment. Inkjet printing parameters were set at 80 V peak actuating voltage
56
57 with 3 μs rise time, 10 μs dwell time and 3 μs fall time at a frequency of 200 Hz, The
58
59
60

1
2
3 rationale for choosing appropriate printing conditions have been discussed in detail
4 elsewhere.¹⁶ The dimensions of printed structures were measured either using
5 conventional optical microscopy or with a white light interferometric system
6 (MicroXAM Surface Mapping Microscope, Phase Shift Technology Inc., Tucson, AZ,
7 USA).

8
9
10
11
12
13
14
15
16
17 Coffee staining behaviour of printed drops was investigated on a range of substrates
18 including: glass microscope slides (BDH, Poole, UK), an epoxy resin (Accura SI 40
19 material, 3D Systems GmbH, Darmstadt, Germany), pre-printed and dried ZrO₂
20 powder layers. To investigate the stability of printed liquid lines made using the 10
21 vol % ZrO₂ ink, we printed using the same conditions as with coffee staining tests but
22 with two different nozzle to substrate relative speeds of 40 mms⁻¹ and 80 mms⁻¹
23 respectively. We printed lines with droplet spacing values in the range from 10 μm
24 to 80 μm to study the morphological stability of the resulting printed lines.
25
26
27
28
29
30
31
32
33
34
35
36
37
38
39
40
41
42
43
44
45
46
47
48
49
50
51
52
53
54
55
56
57
58
59
60

In order to study the stability of drops printed on top of a dried printed ceramic
powder layer, a single ceramic layer, was prepared on an epoxy resin substrate by
inkjet printing a pattern of overlapping drops. Subsequently individual isolated dots
and lines were printed onto the pre-printed layer to allow the study of coffee staining
during multi-layer printing.

Results and Discussion

Ink preparation

To optimize the composition of the ZrO₂ aqueous ink, we have measured the viscosities of 10 vol % suspensions using a range of surfactant dosage. A contour map of the suspensions' viscosity is shown in Figure 1. The viscosity of the ink increases with increasing dosage of surfactant, especially with DOLAPIX CE 64. The optimised composition for the ink is 10 vol % ZrO₂ powder aqueous suspensions with 1 wt % DISPEX A 40 and 0.5 wt % DOLAPIX CE 64. Note that the viscosity values plotted in Figure 1 were taken from samples after identical milling time, but are not the final viscosities of the optimized suspensions. After efficient milling (7 days), the optimized ZrO₂ ink had a viscosity of 2.46 mPas and was suitable for inkjet printing. Sedimentation tests on the inks indicate that the inks were stable over time intervals consistent with printing experiments. After standing for 24h, there is no visible sedimentation with only 4 vol % upper clear water in the ink.

Segregation during drying (Coffee Staining)

Figure 2 shows 3-D reconstruction images obtained from interferometric microscopy data of single droplets of the 10 vol % ZrO₂ ink inkjet printed onto glass substrates and dried. The temperature range of the substrates applied in this study is from 25 °C to 200 °C. At all temperatures there is significant coffee staining with most of the ZrO₂ particles depositing towards the edge of the drop. The diameter of the dried droplet is seen to decrease dramatically when the substrate temperature is increased to 35 °C, but shows little subsequent reduction in radius with further increase in

1
2
3 temperature. The height difference between the droplet edge and centre is found to
4
5 increase with increasing substrate temperature. It has been observed in other work on
6
7 droplet drying that printing onto a heated substrate can result in a reduction in coffee
8
9 staining.^{17,18} However, in this case an increase in temperature has little influence on
10
11 coffee staining, which is consistent with the proposal of Soltman and Subramaian¹⁹
12
13 and the modelling work of Ozawa²⁰ that the heating of the substrate will preferentially
14
15 enhance evaporation close to the contact line and thus increase the driving force for
16
17 coffee staining.
18
19
20
21

22
23
24 In order to investigate the influence of solvent mixtures on coffee staining the
25
26 aqueous solvent was mixed with 10 wt % ethanol or PEG prior to the addition of
27
28 surfactants and ZrO₂. Both ethanol and PEG reduce the surface tension of water with
29
30 increasing concentration but ethanol/water mixtures will preferentially lose ethanol
31
32 through evaporation while PEG/water mixtures will lose water. In which case, we
33
34 expect the influence of differential evaporation to lead to a Marangoni flow that
35
36 opposes coffee staining with the PEG/water solvent mixture and a flow that does not
37
38 impede coffee staining with ethanol/water mixtures. Figure 3 and 4 shows results
39
40 from dried drops obtained from these solvent mixtures after inkjet printing onto glass
41
42 substrates at a range of temperatures.
43
44
45
46
47
48
49

50
51 The behaviour of dried drops obtained using ethanol/water mixtures are shown in
52
53 Figure 3. Coffee staining is still present at all substrate temperatures, however, there
54
55 are significant differences between the behaviour of this mixture and that of pure
56
57 water suspensions (Figure 2). The diameter of the dried drops shows less variation
58
59 with temperature and the width of the deposit at the contact line is increased and its
60

1
2
3 height is reduced. This reduction in the severity of the segregation may indicate that
4
5 the contact line is less well pinned than with the aqueous suspensions and that some
6
7 retraction of the contact line has occurred.
8
9

10
11
12 The behaviour of drops printed using the PEG/water suspensions are shown in Figure
13
14 4. At 25 and 35 °C (Figures 4a and 4b) coffee staining has been eliminated, however,
15
16 at higher substrate temperatures coffee staining and segregation of the dried deposit is
17
18 seen (Figures 4c and 4d). This behaviour is consistent with the expected behaviour of
19
20 the Marangoni effect as quantified by the Marangoni number (Equation 1). Coffee
21
22 staining is opposed by a surface tension driven flow set up by a concentration gradient.
23
24 Diffusion within the liquid droplet will tend to reduce the concentration gradient and
25
26 thus increasing temperature will decrease the value of the Marangoni number because
27
28 of the presence of the diffusion coefficient in the denominator of Equation 1.
29
30 However at room temperature the addition of PEG to the aqueous solution is
31
32 sufficient to prevent coffee staining.
33
34
35
36
37
38
39
40
41

42 *Stability of Printed Surface Features*

43
44 Solid objects are produced by the sequential printing of layers. Each layer is formed
45
46 by a number of overlapping liquid drops that coalesce to form the desired pattern.
47
48 These drops remain on the surface in liquid form until they dry, hence there is a
49
50 period of time when there will be a series of 2-D liquid features that must remain
51
52 stable and maintain their desired shape for a period of time on the surface. The
53
54 stability of liquid sheets has not been researched in great detail. However, there has
55
56 been significant work on the stability of linear liquid features, such as are formed by
57
58 the coalescence of a line of overlapping drops. Davis proposed that liquid linear
59
60

1
2
3 features or beads can be stable on a smooth surface if the contact line is pinned²¹ and
4 this was confirmed experimentally by Schiaffino and Sonin.²² Smith *et al* identified a
5 maximum drop spacing, below that for droplet overlap, above which drops do not
6 form parallel sided liquid tracks.²³ Duineveld observed a minimum drop spacing
7 below which a dynamic instability set in, which results in regular spaced bulges along
8 a liquid track.²⁴ These two instabilities were used by Soltman and Subramanian to
9 propose that there is a limited set of drop spacings between which stable parallel side
10 lines can be formed by inkjet printing.¹⁹
11
12
13
14
15
16
17
18
19
20
21
22
23
24

25 The limit set by the maximum spacing of overlapping drops is shown to be related to
26 the equilibrium behavior of spreading liquid limited by contact line pinning.²³ The
27 minimum drop spacing below which the bulging instability occurs was shown by
28 Duineveld to be a dynamic function of the transverse velocity of the printing device
29 relative to the substrate, U_T .²⁴ In dimensionless form this velocity is
30
31
32
33
34
35
36
37
38
39
40
41
42
43
44
45
46
47
48
49
50
51
52
53
54
55
56
57
58
59
60

$$U_T^* = \frac{\eta U_T}{\sigma_{LV}} \quad (2)$$

where η is the dynamic viscosity of the fluid and σ_{LV} is the liquid/vapor interfacial energy. Stringer developed Duineveld's model¹⁴ to show that stable liquid tracks are formed if the dimensionless velocity is greater than a function of the dimensionless drop spacing, p^* , and the advancing contact angle of the liquid on the substrate, θ_a .

$$U_T^* > g(p^*, \theta_a) \quad (3a)$$

with

$$p^* = \frac{p}{\beta_{eqm} d_0} \quad (3b)$$

where p is the spacing of drops on the substrate, d_0 is the diameter of the original spherical drop and $\beta_{eqm} = d_{eqm}/d_0$ or the ratio between the equilibrium spread diameter of the drop on the substrate, d_{eqm} , and d_0 .¹⁴

Stringer *et al* showed that the function $g(p^*, \theta)$ is related to the inverse of the drop spacing and the contact angle and is given explicitly as Equation 16c in ref. [14]. The fluid property data required for the model is presented in Table 1. A number of tracks were printed with varying amounts of droplet overlap to explore the validity of the model. Two nozzle to substrate transverse speeds (U_T) of 40 mms^{-1} and 80 mms^{-1} were used to investigate printed line stability over a range of drop spacing p in the range $10 \mu\text{m}$ to $100 \mu\text{m}$.

Figure 5 shows optical microscope images of printed lines from both the original aqueous ink and a 10 wt % PEG solution ink. Both inks show similar behavior with parallel sided tracks printed at a drop spacing of $50 \mu\text{m}$. However, at low drop spacing ($30 \mu\text{m}$) a bulging instability was seen (Figures 5a and 5d) and at large drop spacings ($90 \mu\text{m}$) there is insufficient droplet overlap for a stable parallel sided track to form. This behaviour is qualitatively the same as that observed by Soltman and Subramanian for solutions of PEDOT/PSS¹⁹ and by Stringer *et al* with a silvernanoparticle ink.¹⁴ Note that lines printed using the aqueous ink in Figure 5 a, b and c show coffee staining as raised ridges at their edges, while the lines printed with the 10 wt % PEG ink show no effect. Figure 6 shows the predictions of the model derived by Stringer *et al* for the onset of the bulging instability,¹⁴ our experimental

1
2
3 results show excellent agreement.
4
5
6
7

8 ***Multilayer Printing***

9

10 The fabrication of 3-D objects can be achieved by printing second and subsequent
11 layers on top of pre-printed and dried layers. Figure 7 shows single pass printed dots
12 and lines using the 10 wt % PEG ink on an epoxy resin substrate and on a pre-printed
13 layer of dried ZrO₂ powder. The printed objects show no coffee staining on the epoxy
14 resin substrate, but the dots and lines on the pre-printed layer show obvious coffee
15 staining. In both cases the printed features were dried in air at room temperature
16 (approximately 25 °C). Figure 8 shows reconstructed 3-D images and line profiles
17 across printed dot features made from single drops and repeated overprints of 5 and
18 10 drops on both the epoxy resin and the ZrO₂ powder surfaces. In all cases the drops
19 printed on the epoxy resin substrate show a single central peak and dry to form a
20 convex mound, consistent with our previous observation of isolated drops and printed
21 lines. However, when the ink is printed on top of the ZrO₂ powder that had been
22 previously printed, severe coffee staining occurs.
23
24
25
26
27
28
29
30
31
32
33
34
35
36
37
38
39
40
41
42

43 To the best of our knowledge, this is the first report of coffee staining during drop
44 drying on porous substrates. All prior work on coffee staining has considered solvent
45 removal by evaporation and the resulting flows that occur if the contact line is pinned.
46 Because of this focus on evaporation, methods to reduce coffee staining have
47 concentrated on modifying the loss of solvent by evaporation and generating
48 countervailing Marangoni flows. The choice of PEG solutions to reduce coffee
49 staining in this work was guided by these principles and prior work in the literature.
50
51 Thus we hypothesise that the unexpected appearance of coffee staining after printing
52
53
54
55
56
57
58
59
60

1
2
3 on a ZrO_2 powder layer indicates the importance of a second form of solvent removal
4
5 when a drop rests on a porous substrate. In this case solvent removal can occur by
6
7 absorption into the porous media beneath the drop. This route will be drain the liquid
8
9 uniformly and show no differential between transport of the water and PEG. If the
10
11 contact line remains pinned, a differential flow will be required within the drop and
12
13 coffee staining occur as in the case of uniform evaporation.¹² Unlike evaporation
14
15 driven coffee staining, this mechanism will only operate if particles are in suspension
16
17 as any material in solution will be absorbed along with the solvent.
18
19
20
21
22
23
24

25 **Conclusions**

26
27 We have prepared 10 vol % ZrO_2 aqueous suspensions that have low viscosity and
28
29 sufficient stability to be suitable for inkjet printing. However, when individual drops
30
31 and simple linear features are printed, they show significant solute redistribution
32
33 during drying, also known as coffee staining. This coffee staining can be removed on
34
35 solid substrates using appropriate solvent mixtures, which was achieved in this case
36
37 by adding 10 wt % PEG into the original ink. Using the modified ink, coffee staining
38
39 was completely eliminated at room temperature (25 °C), however, at temperatures
40
41 above 35 °C coffee staining was again observed and this can be explained by
42
43 diffusion reducing the concentration gradients that drive Marangoni flow. When
44
45 material was printed onto a layer of dried ceramic powder, coffee staining was found
46
47 at room temperature with the PEG modified ink. This is believed to be because in this
48
49 case the drops dry by the draining of fluid into the dried powder bed. This
50
51 phenomenon may have implications for other applications of printing onto porous
52
53 substrates as well as for ceramic processing.
54
55
56
57
58
59
60

1
2
3
4
5
6 We have also studied the formation of linear features by overlapping printed drops.
7
8 Stable parallel sided lines are formed within a limited range of drop spacing as has
9
10 been reported in the literature for other printed fluids. The minimum drop spacing,
11
12 below which a bulging instability is seen, is found to consistent with the predictions
13
14 of Stringer's model.¹⁴
15
16
17
18
19

20 **References**

- 21
22
23 1) B. Derby and N. Reis, "Inkjet printing of highly loaded particulate suspensions,"
24
25 *MRS Bulletin*, **28** [11] 815-818 (2003).
26
27
28 2) P. Calvert, "Inkjet printing for materials and devices," *Chem. Mater.*, **13** [10] 3299-
29
30 3305 (2001).
31
32
33 3) B. Derby, "Bioprinting: inkjet printing proteins and hybrid cell-containing materials
34
35 and structures," *J. Mater. Chem.*, **18** [47] 5717-5721 (2008).
36
37
38 4) B. Derby, "Inkjet printing of functional and structural materials - fluid property
39
40 requirements, feature stability and resolution", *Ann. Rev. Mater. Res.* **40**, 395-414
41
42 (2010).
43
44
45 5) W. D. Teng, M. J. Edirisinghe, and J. R. G. Evans, "Optimization of dispersion and
46
47 viscosity of a ceramic let printing ink," *J. Amer. Ceram. Soc.*, **80** [2] 486-494 (1997).
48
49
50 6) Q. F. Xiang, J. R. G. Evans, M. J. Edirisinghe, and P. F. Blazdell, "Solid
51
52 freeforming of ceramics using a drop-on-demand jet printer," *Proceedings of the*
53
54 *Institution of Mechanical Engineers Part B-Journal of Engineering Manufacture*, **211**
55
56 [3] 211-214 (1997).
57
58
59 7) C. E. Slade and J. R. G. Evans, "Freeforming ceramics using a thermal jet printer,"
60
Journal of Materials Science Letters, **17** [19] 1669-1671 (1998).

- 1
2
3 8) M. Mott, J. H. Song, and J. R. G. Evans, "Microengineering of ceramics by direct
4 ink-Jet printing," *Journal of the American Ceramic Society*, **82** [7] 1653-1658 (1999).
5
6
7
8 9) K.A.M. Seerden, N. Reis, J.R.G. Evans, P.S. Grant, J.W. Halloran and B. Derby,
9
10 "Inkjet Printing of Wax Based Ceramic Suspensions", *J. Amer. Ceram. Soc.* **84** [11]
11
12 2514-2520 (2001).
13
14
15 10) B. Derby, "Inkjet Printing Ceramics: From Drops to Solid", *J. Europ. Ceram. Soc.*
16
17 In press (2011) [doi:10.1016/j.jeurceramsoc.2011.01.016](https://doi.org/10.1016/j.jeurceramsoc.2011.01.016)
18
19
20 11) R. D. Deegan, O. Bakajin, T. F. Dupont, G. Huber, S. R. Nagel, and T. A. Witten,
21
22 "Capillary flow as the cause of ring stains from dried liquid drops," *Nature*, **389** 827-
23
24 829 (1997).
25
26
27 12) R. D. Deegan, O. Bakajin, T. F. Dupont, G. Huber, S. R. Nagel, and T. A. Witten,
28
29 "Contact line deposits in an evaporating drop", *Phys. Rev. E* **62** [1] 756-65 (2000)..
30
31
32 13) Y. Zhang, L. F. Chen, S. F. Yang, and J. R. G. Evans, "Preparation of ceramic
33
34 well plates for combinatorial methods using the morphogenic effects of droplet
35
36 drying," *J. Amer. Ceram. Soc.* **89** [12] 3858-3860 (2006).
37
38
39 14) J. Stringer and B. Derby, "Formation and Stability of Lines Produced by Inkjet
40
41 Printing," *Langmuir*, **26** [12] 10365-10372 (2010).
42
43
44 15) B. J. de Gans and U. S. Schubert, "Inkjet printing of well-defined polymer dots
45
46 and arrays". *Langmuir* **20** [18] 7789-93 (2004).
47
48
49 16) N. Reis, C. Ainsley, and B. Derby, "Inkjet delivery of particle suspensions by
50
51 piezoelectric droplet ejectors", *J. Appl. Phys.* **97**, 094903 (2005).
52
53
54 17) J. W. Song, J. Kim, Y. H. Yoon, B. S. Choi, J. H. Kim and C. S. Han, "Inkjet
55
56 printing of single-walled carbon nanotubes and electrical characterization of the line
57
58 pattern" *Nanotechnology* **19** [9] 095702 (2008).
59
60

- 1
2
3
4
5
6
7
8
9
10
11
12
13
14
15
16
17
18
19
20
21
22
23
24
25
26
27
28
29
30
31
32
33
34
35
36
37
38
39
40
41
42
43
44
45
46
47
48
49
50
51
52
53
54
55
56
57
58
59
60
- 18) T. Wang, M. A. Roberts, I. A. Kinloch and B. Derby, “Inkjet Printed Carbon Nanotube Networks: The Influence of Drop Spacing and Drying on Electrical Properties”, submitted to *Nanotechnology* (2011).
- 19) D. Soltman and V. Subramanian, “Inkjet-printed line morphologies and temperature control of the coffee ring effect”, *Langmuir* **24** [5] 2224-31 (2008).
- 20) K. Ozawa, E. Nishitani and M. Doi “Modelling of the drying process of liquid droplet to form thin film”, *Japanese Journal of Applied Physics Part 1* **44** [6A] 4229-34 (2005).
- 21) S. H. Davis, “Moving contact lines and rivulet instabilities. 1. The static rivulet”. *J Fluid Mech* **98** [May] 225-42 (1980).
- 22) S. Schiaffino and A. A. Sonin. “Formation and stability of liquid and molten beads on a solid surface”. *J Fluid Mech* **343** [July] 95-110 (1997).
- 23) P. J. Smith, D. Y. Shin, J.E. Stringer, B. Derby and N. Reis. “Direct ink-jet printing and low temperature conversion of conductive silver patterns”. *J Mater Sci* **41** [13] 4153-8 (2006).
- 24) P. C. Duineveld, “The stability of ink-jet printed lines of liquid with zero receding contact angle on a homogeneous substrate.” *J. Fluid Mech.* **477** [Feb] 175–200 (2003).

Figure and Table Captions

Table 1. Physical properties of the printed inks required for the bulging instability model.

Figure 1. Viscosity contour map of the 10 vol % zirconium oxide powder aqueous ink with two different surfactants.

Figure 2. Interferometric microscope images of dried single droplets printed by using the 10 vol % zirconium oxide powder aqueous ink on glass substrates at different temperatures: (a) 25°C; (b) 35°C; (c) 50°C; (d) 75°C; (e) 100°C; (f) 200°C.

Figure 3. Interferometric microscope images of dried single droplets printed by using the 10 vol % zirconium oxide powder aqueous ink with 10 wt % ethanol on glass substrates at different temperatures: (a) 25°C; (b) 35°C; (c) 50°C; (d) 100°C.

Figure 4. Interferometric microscope images of dried single droplets printed by using the 10 vol % zirconium oxide powder aqueous ink with 10 wt % polyethylene glycol on glass substrates at different temperatures: (a) 25°C; (b) 35°C; (c) 50°C; (d) 100°C.

1
2
3 **Figure 5.** Optical microscope images of dried lines printed by using the 10 vol %
4 ZrO₂ aqueous ink (a, b, c) and the ink with 10 wt % PEG (d, e, f) on epoxy resin
5 substrates: (a) $p = 30 \mu\text{m}$, $U_T = 40 \text{ mms}^{-1}$; (b) $p = 50 \mu\text{m}$, $U_T = 40 \text{ mms}^{-1}$; (c) $p =$
6 $90 \mu\text{m}$, $U_T = 40 \text{ mms}^{-1}$; (d) $p = 30 \mu\text{m}$, $U_T = 40 \text{ mms}^{-1}$; (e) $p = 50 \mu\text{m}$, $U_T = 40$
7 mms^{-1} ; (f) $p = 90 \mu\text{m}$, $U_T = 40 \text{ mms}^{-1}$.

8
9
10
11
12
13
14
15
16
17
18 **Figure 6.** Stability map showing the condition for the onset of bulging instability,
19 with data from experiments on our 10 vol % zirconium oxide powder aqueous ink
20 superimposed, together with data from reference¹⁰. In all cases, open symbols indicate
21 unstable morphology and filled symbols indicate stable morphology.

22
23
24
25
26
27
28
29
30 **Figure 7.** Optical microscope images of dots and lines on the epoxy resin substrate
31 and pre-printed layer, which are printed by using the original ink with 10 wt % PEG:
32 (a) a dot on epoxy resin substrate; (b) a dot on the pre-printed layer; (c) a line on
33 epoxy resin substrate; (d) a line on the pre-printed layer.

34
35
36
37
38
39
40
41 **Figure 8.** Interferometric microscope images of dried dots printed by using the 10
42 vol % original ink with 10 wt % PEG by single and multi-passes printing on epoxy
43 resin substrate (left row) and the pre-printed layer (right row).
44
45
46
47
48
49
50
51
52
53
54
55
56
57
58
59
60

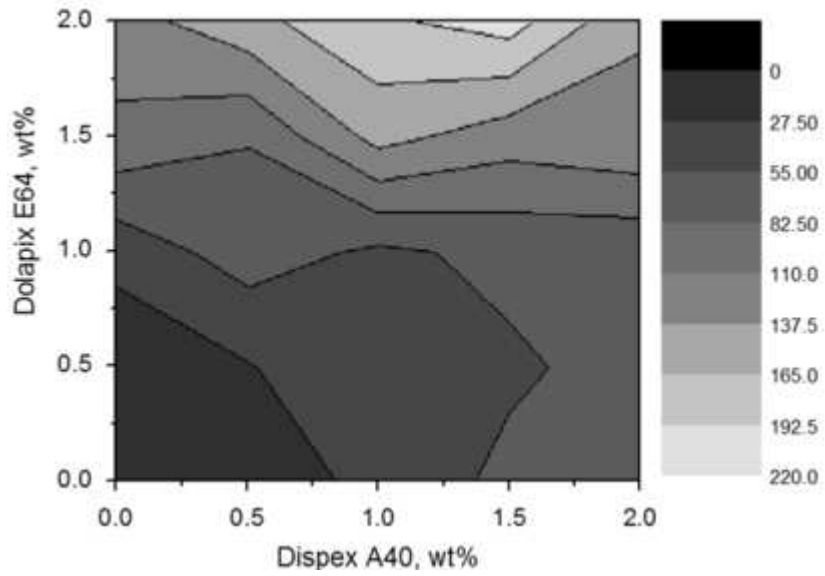
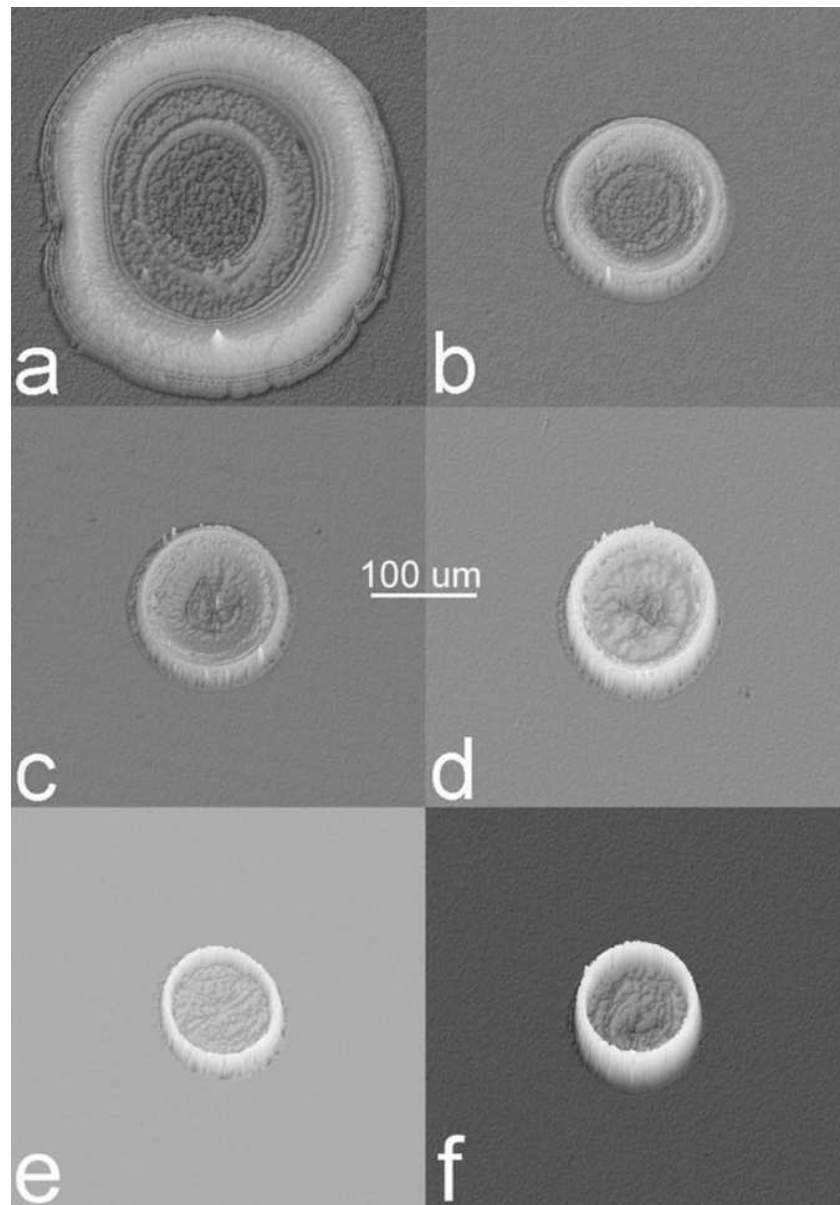


Figure 1. Viscosity contour map of the 10 vol % zirconium oxide powder aqueous ink with two different surfactants.
17x12mm (600 x 600 DPI)

er Review



46
47
48
49
50
51
52
53
54
55
56
57
58
59
60

Figure 2. Interferometric microscope images of dried single droplets printed by using the 10 vol % zirconium oxide powder aqueous ink on glass substrates at different temperatures: (a) 25°C; (b) 35°C; (c) 50°C; (d) 75°C; (e) 100°C; (f) 200°C.
28x40mm (600 x 600 DPI)

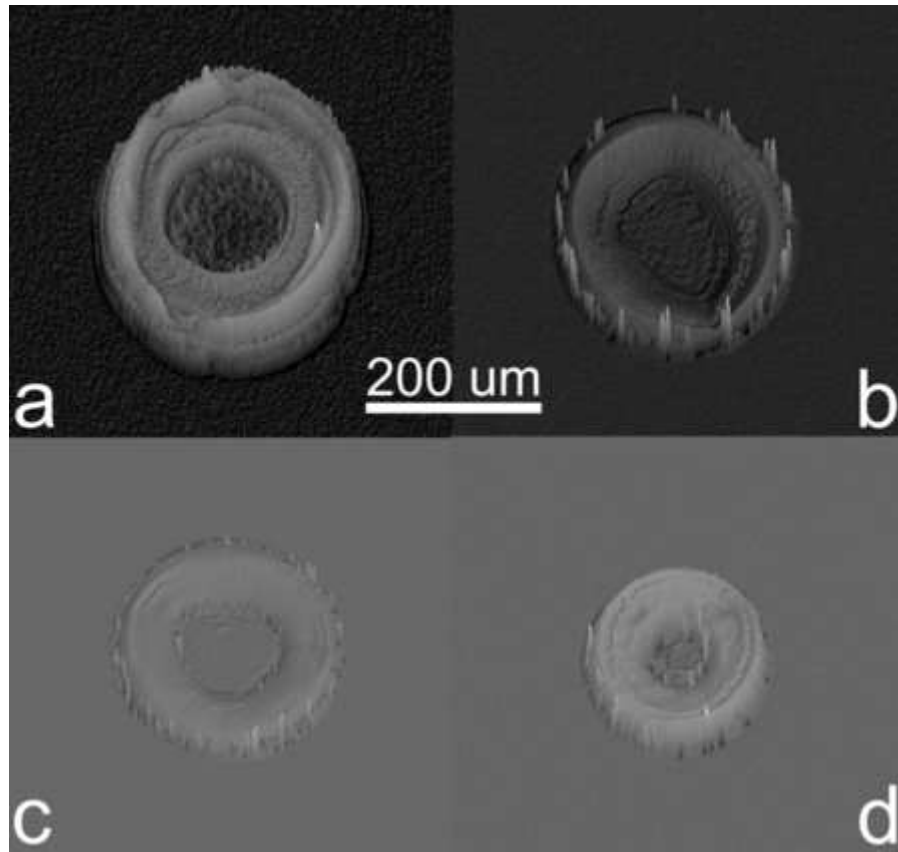


Figure 3. Interferometric microscope images of dried single droplets printed by using the 10 vol % zirconium oxide powder aqueous ink with 10 wt % ethanol on glass substrates at different temperatures: (a) 25°C; (b) 35°C; (c) 50°C; (d) 100°C.
18x17mm (600 x 600 DPI)

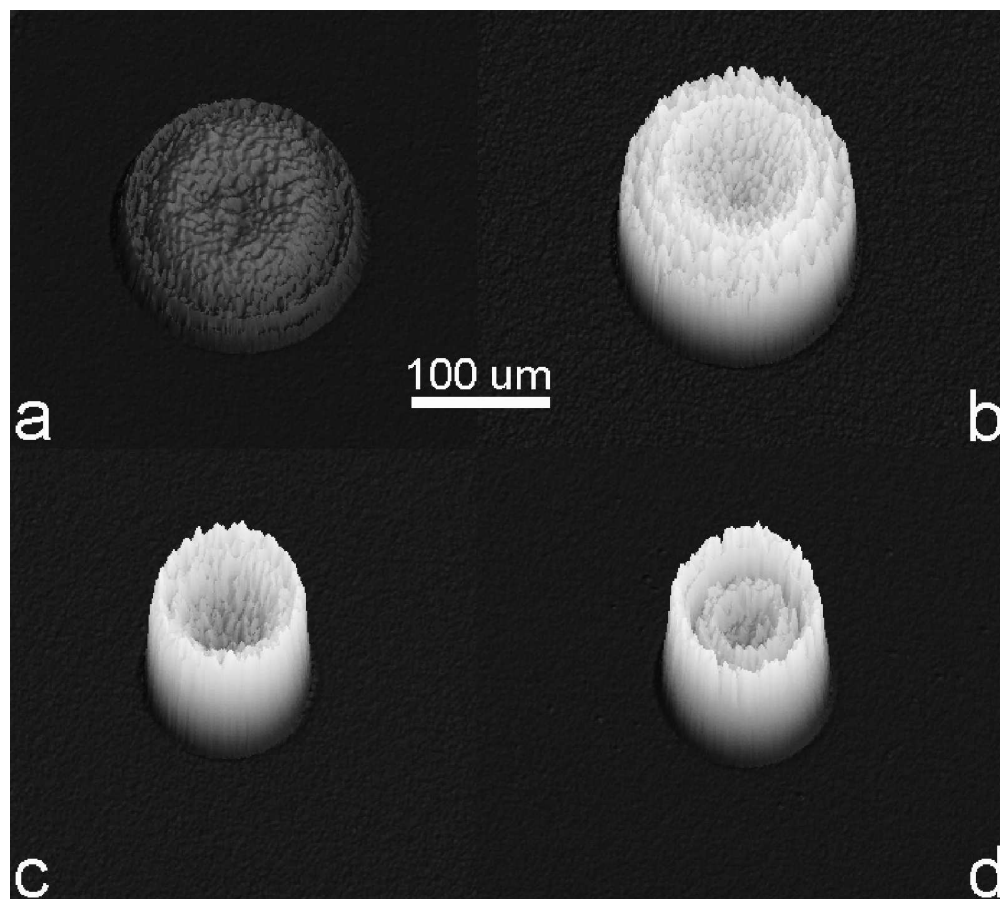


Figure 4. Interferometric microscope images of dried single droplets printed by using the 10 vol % zirconium oxide powder aqueous ink with 10 wt % polyethylene glycol on glass substrates at different temperatures: (a) 25°C; (b) 35°C; (c) 50°C; (d) 100°C.

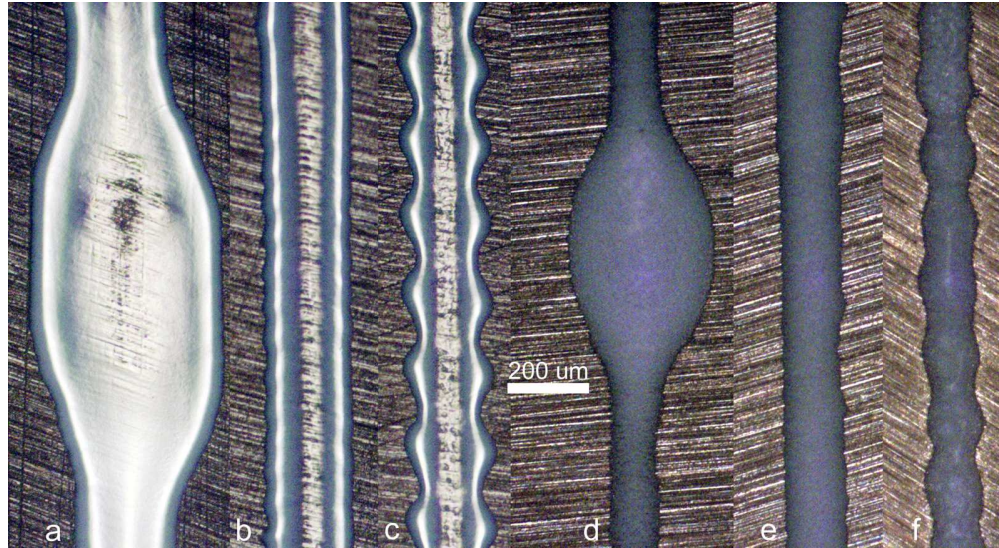


Figure 5. Optical microscope images of dried lines printed by using the 10 vol % ZrO₂ aqueous ink (a, b, c) and the ink with 10 wt % PEG (d, e, f) on epoxy resin substrates: (a) = 30 μm , = 40 mms-1; (b) = 50 μm , = 40 mms-1; (c) = 90 μm , = 40 mms-1; (d) = 30 μm , = 40 mms-1; (e) = 50 μm , = 40 mms-1; (f) = 90 μm , = 40 mms-1.
67x36mm (600 x 600 DPI)

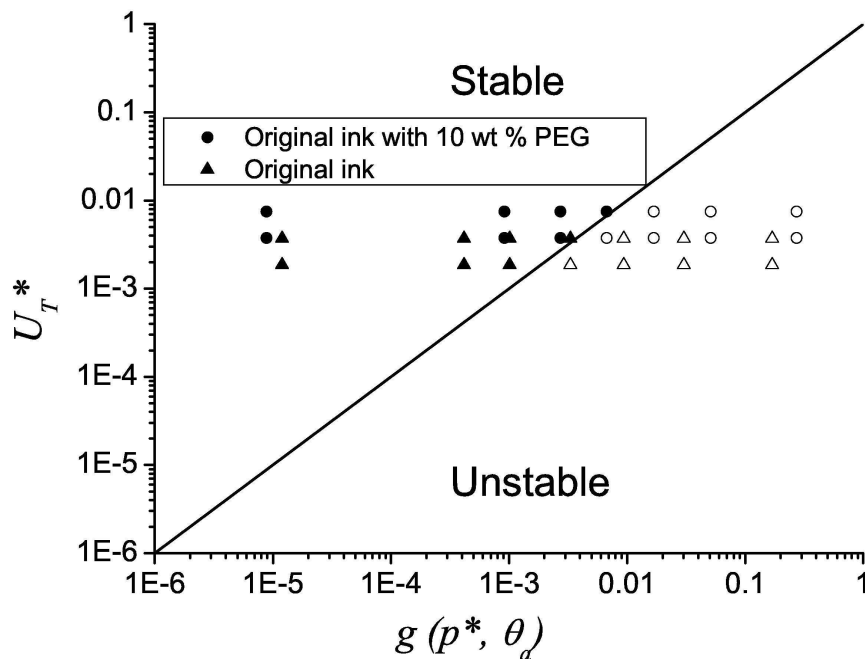


Figure 6. Stability map showing the condition for the onset of bulging instability, with data from experiments on our 10 vol % zirconium oxide powder aqueous ink superimposed, together with data from reference10. In all cases, open symbols indicate unstable morphology and filled symbols indicate stable morphology.
114x87mm (600 x 600 DPI)

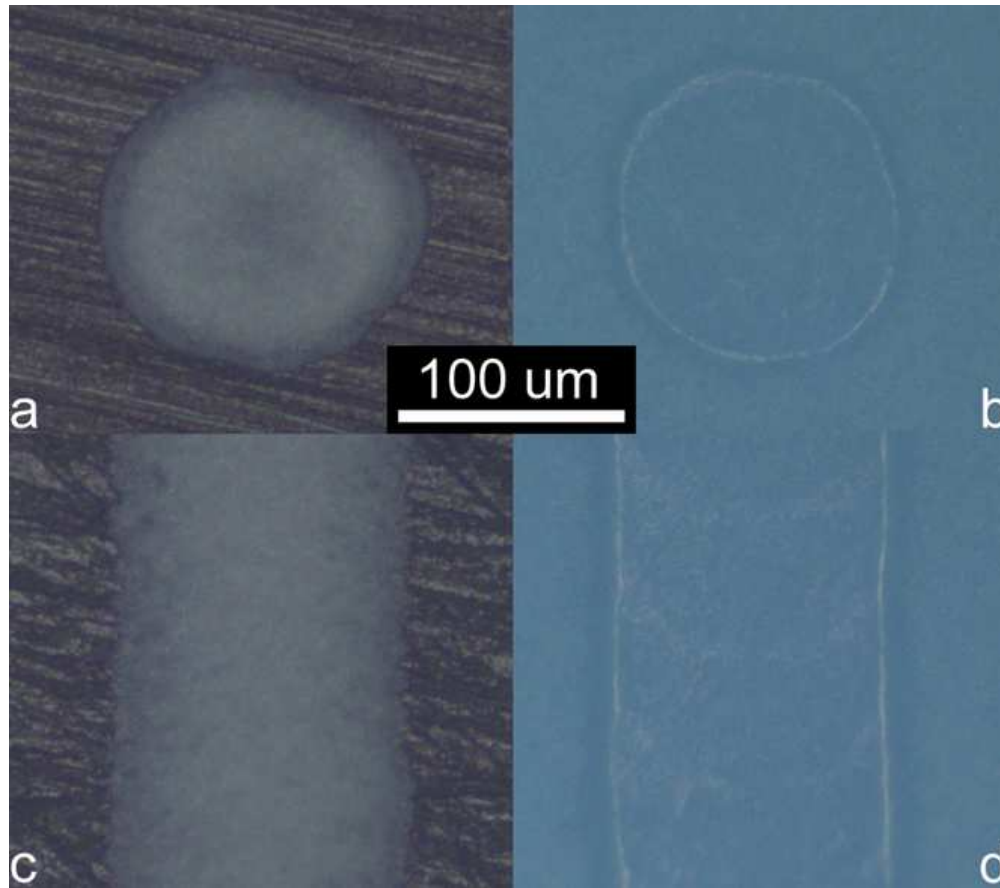


Figure 7. Optical microscope images of dots and lines on the epoxy resin substrate and pre-printed layer, which are printed by using the original ink with 10 wt % PEG: (a) a dot on epoxy resin substrate; (b) a dot on the pre-printed layer; (c) a line on epoxy resin substrate; (d) a line on the pre-printed layer.
28x24mm (600 x 600 DPI)

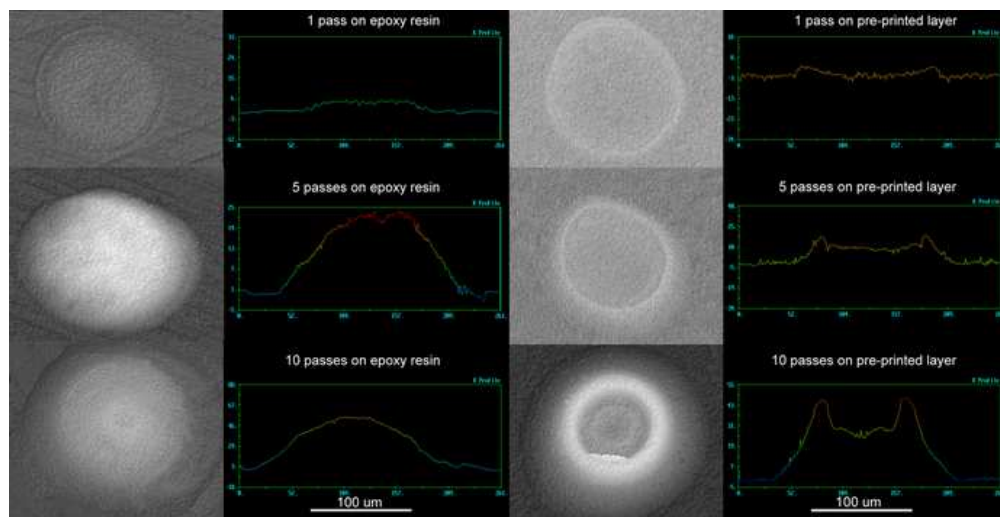


Figure 8. Interferometric microscope images of dried dots printed by using the 10 vol % original ink with 10 wt % PEG by single and multi-passes printing on epoxy resin substrate (left row) and the pre-printed layer (right row).
29x14mm (600 x 600 DPI)

Table 1. Physical properties of the printed inks required for the bulging instability model.

Ink	θ	θ_a	σ_{LV} (mJm ⁻²)	η (mPas)
10 vol % ZrO ₂	56 ± 2.8°	50 ± 1.2°	53	2.46
10 vol % ZrO ₂ /PEG	60 ± 2.6°	53 ± 1.8°	48	4.51

For Peer Review